

KHIFC-user friendly program for studying Heavy ion fusion barrier characteristics

H.C. Manjunatha^{1†}, P.S.Damodara gupta², N.Sowmya^{3‡}, and K.N.Sridhar⁴

¹Department of Physics, Govt. First Grade College, Devanahalli-562110, Karnataka, India

²Department of Physics, Rajah Serfoji Government College, Thanjavur-613005, Affiliated to Bharathidasan University, Tiruchirappalli-TamilNadu

³Department of Physics, Govt. First Grade College, Chikkaballapur-562101, Karnataka, India

⁴Department of Physics, Govt. First Grade College, Malur-563130, Karnataka, India

*Corresponding author : [†]manjunathhc@rediffmail.com, [‡]sowmyaprakash8@gmail.com

June 18, 2025

Abstract

Abstract We have developed an application for studying heavy ion fusion barrier characteristics such as fusion barrier heights (V_B), positions (R_B) and curvature of the inverted parabola ($\hbar\omega$). We call this application as KHIFC (Kolar Heavy Ion fusion barrier Characteristics). This software application hosted in the domain "https://systematics-of-heavy-ion-fusion.vercel.app/". This KHIFC produces fusion cross-sections with the simple input of projectile, target and center of mass energy. The values produced by the KHIFC is validated with experiments. Efficient tools like KHIFC are essential for researchers in nuclear physics, particularly when dealing with complex systems such as actinide and super-heavy nuclei. By providing quick calculations and insights, it can significantly aid in experiment planning and theoretical investigations.

Keywords: fusion barriers, heavy ion, harmonic oscillator

1 PROGRAM SUMMARY

Program title: KHIFC

CPC Library link to program files: <https://data.mendeley.com/datasets/48gwwtfc7z/2>

Licensing provisions: Creative Commons by 4.0 (CC by 4.0)

Programming language: JavaScript, HTML, CSS

Nature of problem: Evaluating the characteristics of the fusion barrier involves a multi-step and complex process that requires careful calculations.

Solution method: By using React with JavaScript, the developed software accepts inputs and evaluates the characteristics of the fusion barrier based on the given input. It also generates graphs to visualize the fusion cross-section data.

2 Introduction

The synthesis of heavy or superheavy nuclei is crucial and is motivated by the theoretical expectation of an "island of stability." These nuclei are the subject of much experimental research, mostly via fusion-evaporation processes [13, 29, 30]. Elements 113 to 118 are among the discoveries made possible by laboratories worldwide. Despite the difficulties in creating and researching these elusive and transient nuclei, the search for superheavy elements is still important and might impact nuclear physics and chemistry. The cold fusion reactions utilize lead and bismuth as targets for $Z=113$ [14, 23, 24, 27], while hot fusion employs ^{48}Ca projectiles with actinide targets for $Z \geq 114$ [31, 32, 33]. Identifying superheavy elements relies on confirming consistent decay chains of the produced compound nucleus.

After the synthesis of superheavy element $Z=118$, many experiments were carried out for the synthesis of superheavy element $Z=119$ and 120 [9, 10]. Additionally, many theoretical models such as dinuclear system model (DNS) [1, 46], Advanced statistical model (ASM) [18, 19], dynamical cluster-decay model [5], dynamical approach based on Langevin equations [40], Time-dependent Hartree-Fock model [39], improved quantum molecular dynamics model [44], fusion-by-diffusion model [41], and many were used in the prediction of evaporation residue cross-sections.

The fusion is a complex process and the cross-sections can vary depending on the specific reaction and conditions involved. To understand the entire fusion process in heavy-ion collisions, (author?) [15] considered the influence of the deformation of both projectile-target nuclei. A comprehensive literature survey reveals theoretical studies focusing on fusion barriers in low and medium atomic number nuclei [2, 26, 35, 38, 42, 43]. In addition many codes such as CASCADE [34], HIVAP [36, 36, 37], CCFUL [8], PACE [7], and POTFUS + GEMINI++ [16] has been used to predict fusion cross-sections. Codes provide estimates of fusion cross-sections as a function of energy and other relevant parameters. The importance of these codes in predicting fusion cross-sections lies in their ability to guide experimental efforts, optimize conditions for fusion reactions, and advance our fundamental understanding of nuclear physics.

Quantum mechanical effects, such as tunneling, play a significant role in nuclear fusion. Tunneling allows nuclei to overcome the Coulomb barrier even when their kinetic energy is insufficient to do so classically. These fusion cross-sections depend sensitively on the energy of the colliding nuclei. Predicting cross-sections across a range of energies requires sophisticated models that account for energy dependence. Hence, this paper aims to address a notable gap in existing literature where references to nuclear codes often lack comprehensive information about the intricacies of the calculations, creating challenges for new users in grasping the inner workings of these codes and discerning their range of applicability. So, the primary objective of this paper is to offer an exhaustive and comprehensive account of each step essential for executing a fusion cross-sections in the actinide and superheavy region, thereby facilitating a thorough understanding for researchers and practitioners entering this domain.

3 Theoretical Framework

In nuclear fusion, the fusion barrier characteristics such as fusion barrier height, barrier position, and the concept of an inverted parabola, are crucial in understanding the dynamics of fusion reactions. The fusion barrier height denotes the energy required for atomic nuclei to overcome electrostatic repulsion during fusion. The barrier position represents the distance where the barrier is maximal, influenced by nuclear forces. An inverted parabola in nuclear fusion depicts the potential energy between colliding atomic nuclei. At close distances, attractive forces prevail, while repulsive forces dominate as nuclei separate. This curve illustrates the energy barrier for fusion reactions, which is crucial for predicting fusion dynamics and optimizing experimental conditions. Further, theoretical formalism for fusion barrier characteristics Actinides [20] and superheavy nuclei [17] were adopted from previous work. The constructed theoretical formalism for active region involves 7205 projectile-target combinations within specified ranges for atomic and mass numbers ($3 < Z_1 < 51, 45 < Z_2 < 100$ and $6 < A_1 < 127, 101 < A_2 < 260$). Where as in case of superheavy nuclei ($104 < Z < 130$), The used theoretical formalism involves 14054 projectile target combinations with atomic and mass number ranges $6 < Z_1 < 58, 52 < Z_2 < 98$ and $12 < A_1 < 142, 120 < A_2 < 252$. The adopted Fusion Characteristics such as fusion barrier heights (V_B), positions (R_B), curvature of the inverted parabola ($\hbar\omega$) are

$$V_B = 1.866 + 1.435 \times \left[\frac{Z_1 Z_2}{R_B} \left(1 - \frac{1}{R_B} \right) \right] \quad (1)$$

$$\begin{aligned} \hbar\omega = & 1.46 \times 10^{-7} \left(\frac{Z_1 Z_2}{A_1^{1/3} + A_2^{1/3}} \right)^3 \\ & - 9.4 \times 10^{-5} \left(\frac{Z_1 Z_2}{A_1^{1/3} + A_2^{1/3}} \right)^2 \\ & + 1.02 \times 10^{-2} \left(\frac{Z_1 Z_2}{A_1^{1/3} + A_2^{1/3}} \right) - 4.02 \end{aligned} \quad (2)$$

Similarly, The adopted Fusion Characteristics for superheavy are

$$\begin{aligned} S_B = & -1.236 \times 10^{-7} \left(\frac{Z_1 Z_2}{A_1^{1/3} + A_2^{1/3}} \right)^3 \\ & + 7.774 \times 10^{-5} \left(\frac{Z_1 Z_2}{A_1^{1/3} + A_2^{1/3}} \right)^2 \\ & - 2.324 \times 10^{-2} \left(\frac{Z_1 Z_2}{A_1^{1/3} + A_2^{1/3}} \right) + 3.759 \end{aligned} \quad (3)$$

$$V_B = 1.4057 \times \left[\frac{Z_1 Z_2}{R_B} \left(1 - \frac{1}{R_B} \right) \right] + 5.4746 \quad (4)$$

$$\begin{aligned} \hbar\omega = & -3.34 \times 10^{-7} \left(\frac{Z_1 Z_2}{A_1^{1/3} + A_2^{1/3}} \right)^3 \\ & + 1.39 \times 10^{-4} \left(\frac{Z_1 Z_2}{A_1^{1/3} + A_2^{1/3}} \right)^2 \\ & - 2.37 \times 10^{-2} \left(\frac{Z_1 Z_2}{A_1^{1/3} + A_2^{1/3}} \right) + 5.67 \end{aligned} \quad (5)$$

We have these fusion barrier characteristics such as fusion barrier heights (V_B), positions (R_B) and curvature of the inverted parabola ($\hbar\omega$) in wong formalism [45] to obtain the fusion cross section;

$$\sigma_{fus} = \frac{(\hbar\omega)(R_B^2)}{0.1E_{cm}} \ln \left(1 + \exp \left[\frac{2\pi}{(\hbar\omega)} (E_{cm} - V_B) \right] \right) \quad (6)$$

4 Results and discussion

The user-friendly, simple computer program KHIFC (Kolar Heavy ion fusion barrier characteristics) is developed for the study of heavy ion fusion systematics based on the theoretical formalism explained in section II. This program produces the fusion barrier characteristics such as fusion barrier height (V_B in MeV), fusion barrier radius (R_B in fm), inverted parabola ($\hbar\omega$ in MeV), fission barrier of the compound nucleus (Bf in MeV), and fusion cross-section. This program will produce the fusion cross section corresponding to input E_{cm} of a wide 100 MeV range. It also gives entrance channel parameters such as the Coulomb interaction parameter, mean fissility, mass asymmetry, charge asymmetry, and isospin number.

The values produced by the present program is validated with the experiments. The fusion barriers and fusion cross

Table 1: Comparison of fusion barriers (MeV) produced by KHIFC with that of the experiments

Reaction	Expt.	KHIFC
$^{16}O + ^{208}Pb \rightarrow ^{224}Th$	74.55 [25]	75.362
$^{19}F + ^{208}Pb \rightarrow ^{227}Pa$	83 [12]	83.763
$^{28}Si + ^{208}Pb \rightarrow ^{236}Cm$	128.1 [11]	128.408
$^{48}Ca + ^{208}Pb \rightarrow ^{256}No$	173.40 ± 0.1 [3]	176.224
$^{54}Cr + ^{208}Pb \rightarrow ^{262}Sg$	207.30 ± 0.3 [3]	210.786
$^{54}Cr + ^{208}Pb \rightarrow ^{262}Sg$	205.8 [21]	210.786
$^{56}Fe + ^{208}Pb \rightarrow ^{264}Hs$	223.00 [6, 21]	228.672
$^{32}S + ^{232}Th \rightarrow ^{264}Ds$	155.73 [6]	158.036
$^{64}Ni + ^{208}Pb \rightarrow ^{272}Ds$	236.00 [6]	243.25
$^{40}Ar + ^{238}U \rightarrow ^{278}Ds$	171.0 [4]	177.352
$^{58}Ni + ^{208}Pb \rightarrow ^{266}Ds$	236.0 [21]	246.725
$^{70}Zn + ^{208}Pb \rightarrow ^{278}Cn$	250.00 [6]	259.018
$^{70}Zn + ^{208}Pb \rightarrow ^{278}Cn$	250.6 [21]	259.018
$^{86}Kr + ^{208}Pb \rightarrow ^{294}Og$	299.00 [6]	308.386
$^{86}Kr + ^{208}Pb \rightarrow ^{294}Og$	303.3 [28]	308.386
$^{84}Kr + ^{232}Th \rightarrow ^{316}126$	332.0 [4]	337.509
$^{84}Kr + ^{238}U \rightarrow ^{322}128$	333.0 [22]	344.623

sections produced by the KHIFC is compared with the experiments. table 1 shows comparison of the fusion barriers produced by the KHIFC with that of the experiments. From this comparison it is observed that the fusion barriers produced by KHIFC is having the percentage of deviation less than 2.5%. This program can be used to produce the fusion barriers of the compound nucleus up to $Z=128$. Furthermore, to validate the fusion-crosssections produced by KHIFC, fusion cross-sections are compared with the experiments and this comparison is shown in fig. 1. For instance, we have selected the fusion reactions such as $^{48}Ca + ^{238}U$, $^{48}Ca + ^{208}Pb$, $^{64}Ni + ^{208}Pb$, and $^{40}Ar + ^{238}U$ and computed the fusion cross-sections using KHIFC. The comparison of experimental fusion cross-sections with that of the KHIFC is validates the fusion cross-sections. From this comparison it is observed that there is a deviation of KHIFC and experiments below the barrier may be due to the fact that deformations effect and angular moment effects are not considered.

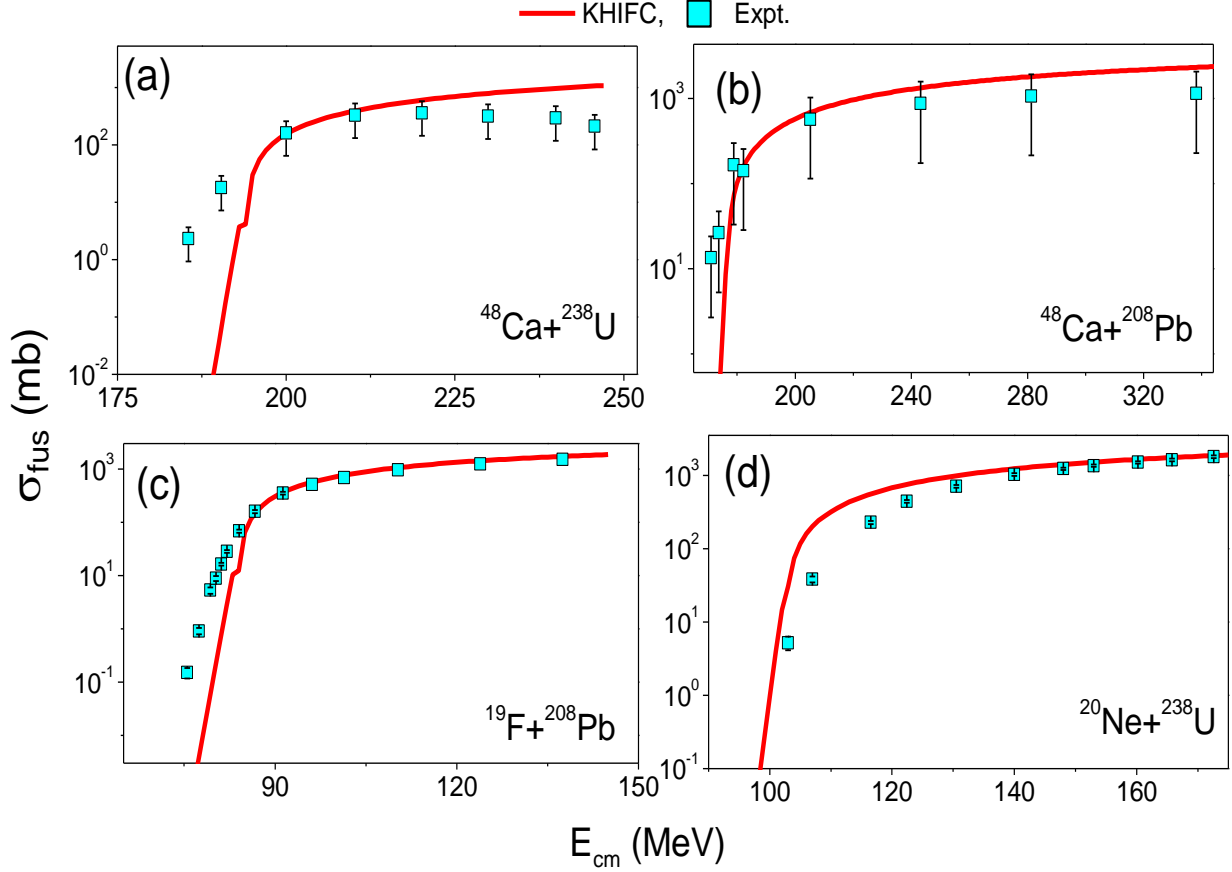


Figure 1: Comparison of fusion cross-section produced by KHIFC with that of the experiments.

4.1 How to use the program

The constructed program is available in website domain "<https://systematics-of-heavy-ion-fusion.vercel.app/>". In the first step, the atomic number and mass number of the projectile and target are required to enter in the first page of the KHIFC. The first page of this program is shown in fig. 2.

After entering the projectile and target atomic and mass numbers enables to press the "calculate" button. The apply of "calculate" button goes to second page which is shown in the fig. 3. This page gives the output of the fusion barrier characteristics such as fusion barrier height (V_B in MeV), fusion barrier radius (R_B in fm), inverted parabola ($\hbar\omega$ in MeV), and fission barrier of the compound nucleus (B_f in MeV).

This KHIFC produces the cross-section in the E_{cm} energy range 100 MeV. Input E_{cm} should be greater than $V_B - 20$ MeV and it can produce fusion cross-sections for the energy range $E_{cm} + 100$ MeV. This program also gives the variation of fusion cross-sections with E_{cm} as a graphical representation which is shown in fig. 4.

Additionally, the fusion cross-sections, calculated using KHIFC, were extended to include superheavy elements with $Z=119$ and 120 . Plots of the fusion cross-sections for the attempted fusion reactions were generated as a function of E_{cm} , depicted in Figure 5(a-b). These cross-sections exhibit an increasing trend, reaching peak values at higher center-of-mass energies. Notably, larger fusion cross-sections were observed for the reactions involving $^{50}\text{Ti} + ^{249}\text{Cf}$ and $^{58}\text{Fe} + ^{244}\text{Pu}$, resulting in the formation of $Z=119$ and $Z=120$ superheavy elements. These insights not only increase our theoretical knowledge of superheavy element synthesis, but they also give important guidance for future experimental work in this area.

5 Summary

We have designed simple user friendly computer program KHIFC which can be used to study the fusion barrier characteristics of actinide and superheavy nuclei with the simple inputs of atomic and mass numbers of projectile, target, and center of mass-energy. This program applies to the atomic and mass number range of projectile $3 < Z_P < 51$,

Kolar Heavy Ion fusion barrier Characteristics

Z_p (Projectile atomic number)

(Please enter in between 6 < Z_p < 52)
A_p (Projectile mass Number)

(Please enter in between 13 < Z_p < 130)
Z_T (Target atomic number)

(Please enter in between 69 < Z_t < 110)
A_T (Target mass Number)

(Please enter in between 120 < Z_p < 252)

Figure 2: Input page of KHIFC

Evaluated Values are

$^{48}\text{Ca} + ^{249}\text{Cf} \rightarrow ^{297}\text{Og}$

Zc : 118
Ac : 297
Vb : 205.435MeV
Rb : 12.693fm
hw : 3.838MeV
Bf : 5.282Mev

Entrance Channel Parameters :

z	X _m	α _Z	η _A
237.72913	0.91195	0.66102	0.67677
Δ(N/Z)	Z ₁ Z ₂	isospin	Z ² /A
0.14082	1960.00000	0.20539	46.88215

Please enter the Ecm for fusion cross section

Fusion Cross Section :

Ecm (MeV)	sfu(mb)

Figure 3: Second page of KHIFC

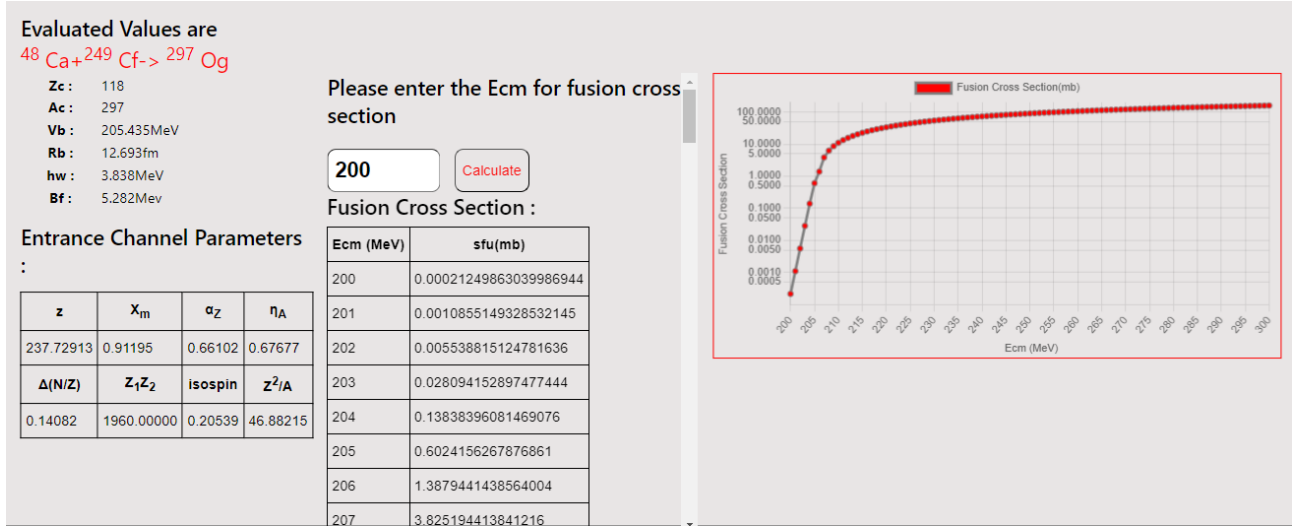


Figure 4: Third page of KHIFC

and $6 < A_1 < 127$ respectively. The target atomic and mass number range varies between $45 \leq Z_T \leq 100$, and $101 \leq A_T \leq 260$ respectively. The program KHIFC is validated with experiments. Eventhough, this program may have certain deviations less than 2.5%, it can be used to study the fusion characteristics quickly. There is a need for quick calculations before planning to the experiments of heavy element synthesis in such cases this program will be useful.

References

- [1] G. G. Adamian, N. V. Antonenko, and W. Scheid. Characteristics of quasifission products within the dinuclear system model. *Physical Review C*, 68(3):034601, 2003.
- [2] R. Arora, R. Puri, and R. Gupta. Analytical calculation of fusion cross-sections. *The European Physical Journal A*, 8:103–114, 2000.
- [3] K. Banerjee, D. J. Hinde, M. Dasgupta, E. C. Simpson, D. Y. Jeung, C. Simenel, B. M. A. Swinton-Bland, E. Williams, I. P. Carter, K. J. Cook, H. M. David, C. E. Düllmann, J. Khuyagbaatar, B. Kindler, B. Lommel, E. Prasad, C. Sengupta, J. F. Smith, K. Vo-Phuoc, J. Walshe, and A. Yakushev. Mechanisms suppressing superheavy element yields in cold fusion reactions. *Phys. Rev. Lett.*, 122:232503, Jun 2019.
- [4] R. Bass. Threshold and angular momentum limit in the complete fusion of heavy ions. *Physics Letters B*, 47(2):139–142, 1973.
- [5] S. Chopra, A. Kaur, and R. K. Gupta. Determination of the compound nucleus survival probability p_{surv} for various “hot” fusion reactions based on the dynamical cluster-decay model. *Physical Review C*, 91(3):034613, 2015.
- [6] I. Dutt and R. K. Puri. Systematic study of the fusion barriers using different proximity-type potentials for $n = z$ colliding nuclei: New extensions. *Phys. Rev. C*, 81:044615, Apr 2010.
- [7] A. Gavron. Statistical model calculations in heavy ion reactions. *Physical Review C*, 21(1):230, 1980.
- [8] K. Hagino, N. Rowley, and A. Kruppa. A program for coupled-channel calculations with all order couplings for heavy-ion fusion reactions. *Computer Physics Communications*, 123(1-3):143–152, 1999.
- [9] J. H. Hamilton, S. Hofmann, and Y. T. Oganessian. Search for superheavy nuclei. *Annual Review of Nuclear and Particle Science*, 63:383–405, 2013.
- [10] F. Heßberger, S. Hofmann, D. Ackermann, V. Ninov, M. Leino, G. Münzenberg, S. Saro, A. Lavrentev, A. Popeko, A. Yeremin, et al. Decay properties of neutron-deficient isotopes 256, 257 db, 255 rf, 252, 253 lr. *The European Physical Journal A-Hadrons and Nuclei*, 12(1):57–67, 2001.
- [11] D. Hinde, C. Morton, M. Dasgupta, J. Leigh, J. Mein, and H. Timmers. Competition between fusion-fission and quasi-fission in the reaction $^{28}\text{Si} + ^{208}\text{Pb}$. *Nuclear Physics A*, 592(2):271–289, 1995.
- [12] D. J. Hinde, A. C. Berriman, M. Dasgupta, J. R. Leigh, J. C. Mein, C. R. Morton, and J. O. Newton. Limiting angular momentum for statistical model description of fission. *Phys. Rev. C*, 60:054602, Sep 1999.

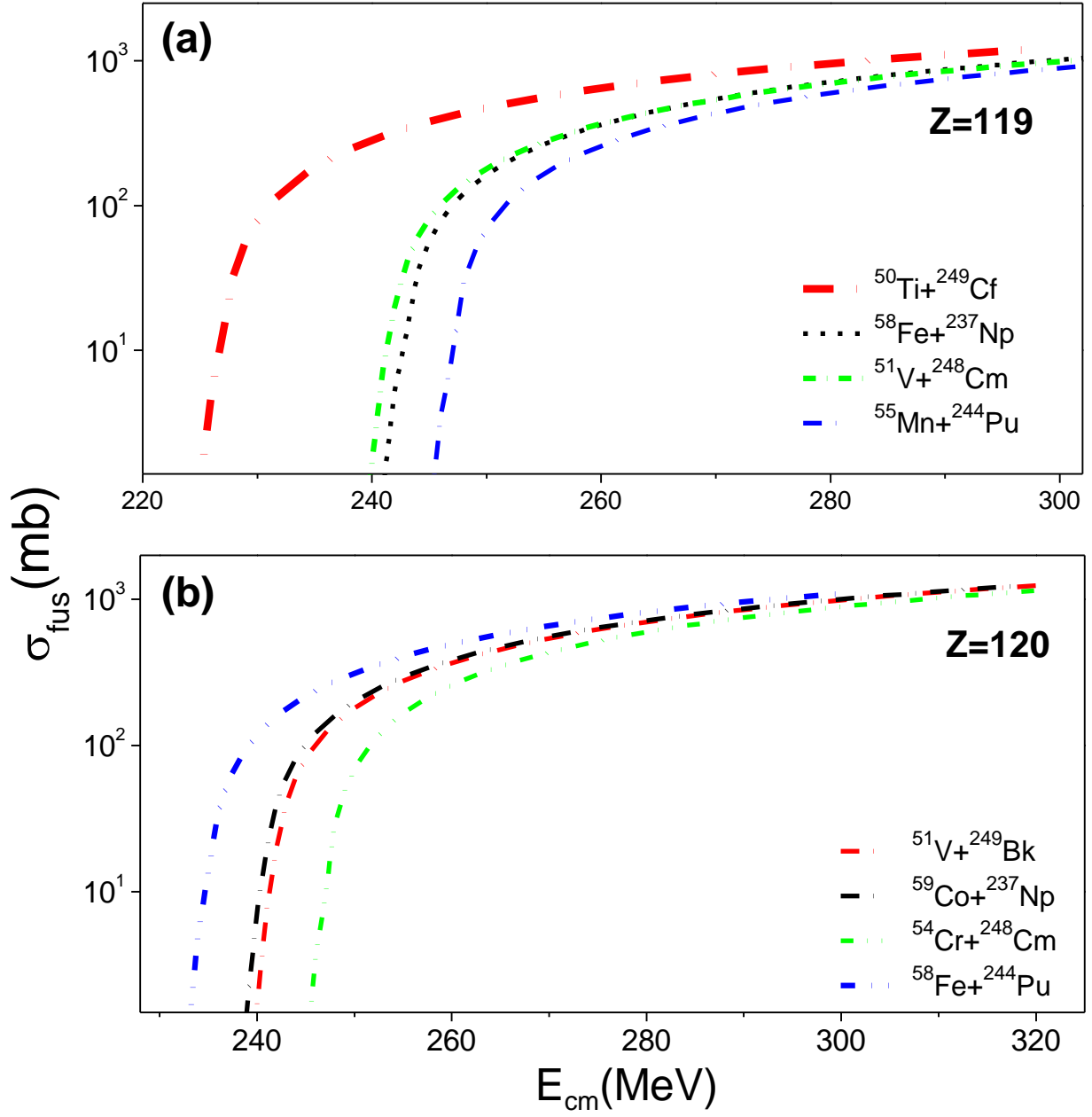


Figure 5: Predicted fusion cross-sections for the synthesis of superheavy element (a) Z=119 and (b) 120 using different fusion cross-sections.

- [13] S. Hofmann, V. Ninov, F. P. Hessberger, P. Armbruster, and H. Folger. G. Münzenberg. *Rev. Mod. Phys.*, 72:733, 2000.
- [14] S. Hofmann, V. Ninov, F. P. Heßberger, P. Armbruster, H. Folger, G. Münzenberg, H. J. Schött, A. G. Popeko, A. V. Yeremin, A. N. Andreyev, et al. Production and decay of $^{269}110$. *Zeitschrift für Physik A Hadrons and Nuclei*, 350:277–280, 1995.
- [15] A. Iwamoto, P. Möller, J. Rayford, H. Sagawa, et al. Collisions of deformed nuclei: A path to the far side of the superheavy island. *Nuclear Physics A*, 596(2):329–354, 1996.
- [16] D. Mancusi, J. Cugnon, A. Boudard, S. Leray, and R. Charity. Comparison between the smm and gemini++ de-excitation models. In *Proc. Satellite Meeting on Nuclear Spallation Reactions, International Topical Meeting on Nuclear Research Applications and Utilization of Accelerators 2009*, 2009.
- [17] H. Manjunatha, K. Sridhar, N. Nagaraja, and N. Sowmya. Pocket formula for fusion barriers of superheavy nuclei. *The European Physical Journal Plus*, 133:1–9, 2018.
- [18] H. C. Manjunatha, N. Sowmya, P. D. Gupta, L. Seenappa, and T. Nandi. Role of optimal beam energies in the heavy ion fusion reaction. *The European Physical Journal Plus*, 137(6):693, 2022.
- [19] H. C. Manjunatha, N. Sowmya, N. Manjunatha, P. S. D. Gupta, L. Seenappa, K. N. Sridhar, T. Ganesh, and T. Nandi. Entrance channel dependent hot fusion reactions for superheavy element synthesis. *Physical Review C*, 102(6):064605, 2020.
- [20] H. C. Manjunatha and K. N. Sridhar. Fusion barrier characteristics of actinides. *Nuclear Physics A*, 971:83–94, 2018.
- [21] S. Mitsuoka, H. Ikezoe, K. Nishio, K. Tsuruta, S. C. Jeong, and Y. Watanabe. Barrier distributions derived from quasielastic backscattering of ^{48}Ti , ^{54}Cr , ^{56}Fe , ^{64}Ni , and ^{70}Zn projectiles on a ^{208}Pb target. *Phys. Rev. Lett.*, 99:182701, Nov 2007.
- [22] L. Moretto. Shell-model calculations of fission decay widths and probabilities in superheavy nuclei. *Nuclear Physics A*, 180(2):337–362, 1972.
- [23] K. Morita, K. Morimoto, D. Kaji, S. Goto, H. Haba, E. Ideguchi, R. Kanungo, K. Katori, H. Koura, H. Kudo, et al. Status of heavy element research using garis at riken. *Nuclear Physics A*, 734:101–108, 2004.
- [24] K. Morita, K. Morimoto, D. Kaji, H. Haba, K. Ozeki, Y. Kudou, T. Sumita, Y. Wakabayashi, A. Yoneda, K. Tanaka, et al. New result in the production and decay of an isotope, $^{278}113$, of the 113th element. *journal of the physical society of japan*, 81(10):103201, 2012.
- [25] C. R. Morton, A. C. Berriman, M. Dasgupta, D. J. Hinde, J. O. Newton, K. Hagino, and I. J. Thompson. Coupled-channels analysis of the $^{16}\text{O}+^{208}\text{Pb}$ fusion barrier distribution. *Phys. Rev. C*, 60:044608, Aug 1999.
- [26] R. Moustabchir and G. Royer. Analytic expressions for the proximity energy, the fusion process and the α emission. *Nuclear Physics A*, 683(1-4):266–278, 2001.
- [27] G. Münzenberg, W. Reisdorf, S. Hofmann, Y. Agarwal, F. Heßberger, K. Poppensieker, J. Schneider, W. Schneider, K. H. Schmidt, H. J. Schött, et al. Evidence for element 109 from one correlated decay sequence following the fusion of 58 fe with 209 bi. *Zeitschrift für Physik A Atoms and Nuclei*, 315:145–158, 1984.
- [28] S. Ntshangase, N. Rowley, R. Bark, S. Förtsch, J. Lawrie, E. Lawrie, R. Lindsay, M. Lipoglavsek, S. Maliage, L. Mudau, S. Mullins, O. Ndwandwe, R. Neveling, G. Sletten, F. Smit, and C. Theron. Barrier distribution for a ‘superheavy’ nucleus–nucleus collision. *Physics Letters B*, 651(1):27–32, 2007.
- [29] Y. Oganessian. Heaviest nuclei from 48ca-induced reactions. *Journal of Physics G: Nuclear and Particle Physics*, 34(4):R165, 2007.
- [30] Y. T. Oganessian. Synthesis and decay properties of heaviest nuclei with 48ca-induced reactions. *Nuclear Physics A*, 787(1-4):343–352, 2007.
- [31] Y. T. Oganessian, F. S. Abdullin, C. Alexander, J. Binder, R. A. Boll, S. N. Dmitriev, J. Ezold, K. Felker, J. M. Gostic, R. Grzywacz, et al. Production and decay of the heaviest nuclei $^{293}113$, $^{294}113$ and $^{294}115$. *Physical review letters*, 109(16):162501, 2012.
- [32] Y. T. Oganessian, F. S. Abdullin, S. Dmitriev, J. M. Gostic, J. H. Hamilton, R. A. Henderson, M. G. Itkis, K. J. Moody, A. N. Polyakov, A. V. Ramayya, et al. New insights into the am $^{243}+^{48}\text{Ca}$ reaction products previously observed in the experiments on elements 113, 115, and 117. *Physical Review Letters*, 108(2):022502, 2012.

- [33] Y. T. Oganessian, V. K. Utyonkov, Y. V. Lobanov, F. S. Abdullin, A. N. Polyakov, I. V. Shirokovsky, Y. S. Tsyganov, G. Gulbekian, S. L. Bogomolov, B. N. Gikal, et al. Measurements of cross sections for the fusion-evaporation reactions $^{244}\text{Pu} + ^{48}\text{Ca}$ \rightarrow $^{292}\text{x} + ^{114}\text{n}$ and $^{245}\text{Cm} + ^{48}\text{Ca}$ \rightarrow $^{293}\text{x} + ^{116}\text{n}$. *Physical Review C*, 69(5):054607, 2004.
- [34] F. Pühlhofer. On the interpretation of evaporation residue mass distributions in heavy-ion induced fusion reactions. *Nuclear Physics A*, 280(1):267–284, 1977.
- [35] R. K. Puri and R. K. Gupta. Fusion barriers using the energy-density formalism: Simple analytical formula and the calculation of fusion cross sections. *Physical Review C*, 45(4):1837, 1992.
- [36] W. Reisdorf. Analysis of fissionability data at high excitation energies: I. the level density problem. *Zeitschrift für Physik A Atoms and Nuclei*, 300(2-3):227–238, 1981.
- [37] W. Reisdorf, F. Hessberger, K. D. Hildenbrand, S. Hofmann, G. Münzenberg, K.-H. Schmidt, W. Schneider, K. Sümmerner, G. Wirth, J. Kratz, et al. Fusability and fissionability in ^{86}Kr -induced reactions near and below the fusion barrier. *Nuclear Physics A*, 444(1):154–188, 1985.
- [38] B. Sahu and C. S. Shastri. Asymmetric parabolic effective barrier model for heavy ion fusion and its relation to coupled channel effects. *Journal of Physics G: Nuclear and Particle Physics*, 25(9):1909, 1999.
- [39] K. Sekizawa and K. Hagino. Time-dependent hartree-fock plus langevin approach for hot fusion reactions to synthesize the $z = 120$ superheavy element. *Physical Review C*, 99(5):051602, 2019.
- [40] C. Shen, G. Kosenko, and Y. Abe. Two-step model of fusion for the synthesis of superheavy elements. *Physical Review C*, 66(6):061602, 2002.
- [41] K. Siwek-Wilczyńska, T. Cap, M. Kowal, A. Sobieczewski, and J. Wilczyński. Predictions of the fusion-by-diffusion model for the synthesis cross sections of $z = 114$ – 120 elements based on macroscopic-microscopic fission barriers. *Physical Review C*, 86(1):014611, 2012.
- [42] A. M. Stefanini, G. Fortuna, R. Pengo, W. Meczynski, G. Montagnoli, L. Corradi, A. Tivelli, S. Beghini, C. Signorini, S. Lunardi, et al. Heavy-ion fusion below the coulomb barrier: The systems $^{28}\text{Si} + ^{58, 62, 64}\text{Ni}$ and $^{32, 34, 36}\text{S} + ^{58, 64}\text{Ni}$. *Nuclear Physics A*, 456(3):509–534, 1986.
- [43] L. C. Vaz, J. M. Alexander, and G. R. Satchler. Fusion barriers, empirical and theoretical: Evidence for dynamic deformation in subbarrier fusion. *Physics reports*, 69(5):373–399, 1981.
- [44] N. Wang, Z. Li, X. Wu, J. Tian, Y. Zhang, and M. Liu. Further development of the improved quantum molecular dynamics model and its application to fusion reactions near the barrier. *Physical Review C*, 69(3):034608, 2004.
- [45] C. Wong. Interaction barrier in charged-particle nuclear reactions. *Physical Review Letters*, 31(12):766, 1973.
- [46] L. Zhu, Z.-Q. Feng, and F.-S. Zhang. Production of heavy neutron-rich nuclei in transfer reactions within the dinuclear system model. *Journal of Physics G: Nuclear and Particle Physics*, 42(8):085102, 2015.